

Design and Testing Of A Hybrid Vertical Axis Wind Turbine for Power Generation

John O. Akande¹, Buhari Mamuda², Zakari M. Salis²

¹Department of Physics, Federal College of Education (Technical) Gusau, Zamfara State, Nigeria

²Department of Science Laboratory Technologies, Federal Polytechnic, Kaura Namoda, Zamfara State, Nigeria

Corresponding Author's Email: mamudabuhari@gmail.com

Received on: October, 2025

Revised and Accepted on: November, 2025

Published on: December, 2025

ABSTRACT

There is a pronounced environmental urgency regarding the need to mitigate the hazards associated with carbon emissions and various pollutants resulting from the incineration of fossil fuels. The foremost approach to achieving this objective involves the utilization of alternative energy sources, among which wind energy is categorized; this energy is harnessed through the implementation of wind turbines. Wind turbines, also referred to as aerogenerators, are sophisticated devices that convert the kinetic energy derived from wind into electrical energy. This research delineates the wind assessment, design, optimization, fabrication, and performance evaluation of a hybrid vertical axis wind turbine (VAWT) aimed at power generation in the Kebbi, Sokoto, and Zamfara states over a two-decade period spanning from 1999 to 2024. Wind data was collected from the Nigeria Meteorological Agency (NIMET) for wind assessment. The design of the hybrid VAWT will be executed utilizing solid modeling tools and SolidWorks software in conjunction with Google SketchUp software, and the fabrication will occur locally. The constructed hybrid VAWT prototype will undergo laboratory testing employing ventilation fans across a spectrum of wind speeds. The VAWTs were tested at four different wind speeds ($V = 4.80$ m/s, 4.50 m/s, 4.30 m/s, and 3.90 m/s). The superior performance of the hybrid VAWT was demonstrated through a direct comparison with the conventional H-Darrieus VAWT under identical experimental conditions. The result revealed that rotational speed and mechanical power have an improvement on the same experimental conditions for hybrid VAWT as (11.0 %, 28.6%, 75.0 %, 14.0 %) and (100 %, 45.5 %, 9.4%, and 40.3 %), respectively, compared to that of H-Darrieus VAWT. The percentage increase demonstrated that the hybrid vertical-axis wind turbine exhibited a substantial enhancement in performance when juxtaposed with the traditional vertical-axis wind turbine. The integration of the Icewind rotor (Savonius Rotor) with the H-Darrieus vertical-axis wind turbine (hybrid VAWT) results in superior self-starting capabilities and enhanced performance across the evaluated parameters in comparison to the standard H-Darrieus vertical-axis wind turbine.

Keywords: Hybrid VAWTs, Darrieus rotor, Savonius rotor, self-starting, efficiency

1.0 INTRODUCTION

The suboptimal efficacy of wind turbines in urban environments can be ascribed to two primary factors: the design of wind turbines that fails to account for the intricate characteristics of the wind resource at the rooftop level, and the inadequate positioning of wind turbines on top of the rooftops. To mitigate these challenges, there is a pressing necessity for an optimized design of wind turbines that is economically viable, straightforward to fabricate in diverse dimensions and energy outputs, and capable of functioning proficiently in locales characterized by complex wind direction. Consequently, many contemporary investigations have underscored the importance of designing wind turbines specifically tailored for urban contexts (Mohammed et al., 2021).

The phenomenon of wind is typically characterized as a significant large-scale movement of air masses within the atmospheric system, or as global air movements

predominantly instigated by pressure differentials that arise from the solar heating of the Earth's atmospheric layer. (Fan et al., 2021; Obada et al., 2024).

Wind turbines, consequently, harness the kinetic energy present in the atmosphere and transform it into rotational mechanical energy, which is then converted into electrical energy (Chaudhuri et al., 2022; Methal et al., 2022).

According to Kumar (Akeremi et al., 2023; Didane et al., 2024), the Darrieus turbine lacks sufficient lift to produce the torque needed to overcome inertia and drive train resistance, failing to initiate rotation at very low wind speeds. Relying solely on lift force to generate torque at low wind speeds is unrealistic for the Darrieus wind turbines. Previous studies have supported this point with wind tunnel tests and field experiments. Due to low lift, a significant drag force is generated, which can produce torque even at low wind speeds, similar to the Savonius

rotor. Building-integrated wind turbines are considered part of a group of technologies suitable for small-scale domestic energy production. This research will focus on designing, fabricating, and experimentally testing the performance of Vertical Axis Wind Turbines (VAWT) on residential buildings (Mohammed et al., 2021). There are various types of wind turbines, but this study concentrates on the design and performance evaluation of hybrid vertical-axis wind turbines for power generation in some northwestern states. This will be achieved through design of turbines (i.e both hybrid and H-Rotor), construction of turbines and performance of these turbines.

2.0 LITERATURE REVIEW

2.1 Hybrid Vertical Axis Wind Turbine (Savonius -Darrieus)

The design combines the Darrieus and Savonius to leverage the strengths of each model. The Darrieus configuration is designed to show a high power coefficient and generally performs better than other vertical-axis wind turbine (VAWT) designs; however, it cannot start on its own (Mojica et al., 2019). On the other hand, the Savonius design has a high starting torque and can start by itself, but it operates at low rotational speeds and has a lower power coefficient. Hybrid designs blend

features from both the Darrieus and Savonius to achieve self-starting ability, high starting torque, and better efficiency. Usually, this hybrid is built as a Darrieus turbine with a drag-type blade in the center, but it is less efficient after startup than a standard lift-type turbine because the central part causes negative drag (Gwani et al., 2020).

Hybrid wind turbines in the evolution of vertical-axis wind turbines (VAWTs) represent the most recent advancement of wind turbines (Mohammed et al., 2022). A hybrid wind turbine converges the characteristics of both Savonius and Darrieus wind turbines within a singular vertical-axis wind turbine framework. This turbine harnesses two forces during its rotation: the drag force attributed to the Savonius wind turbine, which facilitates self-starting, and the lift force generated by the blades of the Darrieus wind turbine, which serves to enhance the rotational velocity of the turbine (Methal et al., 2022).

According to Hidayanti *et al.* (2020), the hybrid wind turbine design is a combination of two-blade Savonius wind turbines and three-bladed Darrieus wind turbines with a diameter of 29.0 cm, a height of 32.0 cm, and a turbine weight of 330.7 g, as shown in Figure 2.1.



Figure 2.1: Hybrid Wind Turbine (Savonius -Darrieus) (Hidayanti *et al.*, 2020)

2.2 Wind speed

According to the blades of a wind turbine undergo rotation due to the kinetic energy imparted by the wind, which is characterized by the wind's velocity. An object possessing mass (m) that traverses at a velocity (v) possesses kinetic energy in the atmosphere, as delineated by

$$E = \frac{1}{2}mv^2 \quad (2.1)$$

2.3 Vertical Axis Wind Turbine: The Swept Area

As articulated by Mamuda, Ahmad & Isah (2020) and Salazar Marin & Rodríguez (2019), in the context of a Vertical Axis Wind Turbine (VAWT), the area is contingent upon both the diameter of the turbine and the height (length) of its blades. For an H-type VAWT, the swept area is determined utilizing the formula represented in equation (2.2), wherein H signifies the turbine's height, and D denotes its diameter.

$$A_s = H \times D \quad (2.2)$$

2.4 Wind power

Wind power serves as a metric for quantifying the volume of wind energy traversing a specified area within a given temporal context. In other terms, wind power constitutes the flux of wind energy across an area of interest (Kalmikov, 2017). As posited by Homzah et al. (2021), the power available in the wind, denoted as P_w , can be expressed mathematically as

$$P_w = \frac{1}{2}\rho Av^3 \quad (2.3)$$

2.5 Turbine Power

The power output generated by the wind turbine is articulated as follows:

$$P_t = \rho Av^3 \eta_t \eta_g \quad (2.4)$$

Where: P = Power output (W), A = Swept area (m^2), ρ = Air density (kg/m^3), v = Wind velocity (m/s), η_t = Wind turbine efficiency, η_g = Generator efficiency

Electrical power can be represented as

$$P_E = \omega \times \tau \quad (2.5)$$

Where ω is the generator speed, and τ is the electromagnetic torque, which is equivalent to the generator torque reference as dictated by the wind turbine controller (Wiens et al., 2021). Moreover, electric power can be calculated using

$$P = I \times V \quad (2.6)$$

Where I represents the current and v denotes the voltage produced by the generator (Sarkar et al., 2020)

2.6 Air Density

According to Dupré et al. (2019), the air density ρ is derived from the temperature T , molar mass M , ideal gas constant R , and pressure P , in accordance with the principles of the ideal gas law:

$$\rho = \frac{MP}{RT} \quad (2.7)$$

The density of the wind has a direct impact on the power output generated by the wind power generator. The mean value of air density is established at 1.225 kg/m^3 (Lester, 2018).

2.7 The Coefficient of Power

In accordance with the Betz limit, the coefficient of power, C_p , max, is theoretically constrained to a maximum value of $16/27$. This value represents the singular maximum rotor power coefficient attainable. The theoretical coefficient of power for a horizontal wind turbine, as elucidated by Betz theory, achieves its peak at $C_p = 0.593$, with actual turbines invariably exhibiting lower values.

The coefficient of power, C_p , which quantifies the efficiency of a wind turbine, can be computed through the equation presented in (2.8) (Mohammed et al., 2021).

$$C_p = \frac{P_t}{0.5\rho AV^3} \quad (2.8)$$

2.8 Torque Coefficient

Torque, or circumferential force, is contingent upon the rated power of the wind turbine and the rotational speed of the rotor, which facilitates the rotation of the turbine about its axis, as described by equation (2.9).

$$C_t = \frac{T}{0.5\rho AV^2 R} \quad (2.9)$$

Here, T represents the torque produced, A signifies the swept area in the wind stream's path, R denotes the radius of the rotor, and V is the free stream velocity (Ali et al., 2020).

3.0 METHODOLOGY

3.1 Study Area

The study area includes Sokoto, Kebbi, and Zamfara States, which are located between Latitude $30^{\circ}35'E$ to $70^{\circ}E$ and Longitude $10^{\circ}N$ to $40^{\circ}N$ in the semi-arid region of Nigeria. The region experiences two distinct seasons each year: the dry season from October to April and the rainy season from May to September (Ayodele et al., 2019).



Figure 2.2: Map of Nigeria Showing the Study Area (Ayodele et al., 2019)

Table 3.1: Monthly mean Wind Speeds for (1988-2024) of Sokoto, Kebbi, and Zamfara States

Month	Jan.	Feb.	Mar.	Apr.	May	Jun.	Jul.	Aug.	Sep.	Oct.	Nov.	Dec.
Wind Speed (m/s)	5.01	4.93	5.32	5.31	5.24	4.83	4.70	4.54	4.23	4.41	4.41	5.14

The annual mean wind speed for the thirty-six years (1988-2024) is 4.87 m/s (NIMET).

The analytical parameters pertaining to the design of the turbine were utilized to develop the hybrid vertical axis wind turbine and its respective components by employing the solid tools of Google SketchUp 2007 model, thereby facilitating the generation of a visual representation complete with dimensional specifications. Initially, the blade was conceptualized employing the tools available in Google SketchUp software, followed by the design of the shaft, Icewind rotor, and radial arm utilizing the same software suite. Subsequently, the rotor support frames (stand) and generator were designed independently. Thereafter, the shaft was inserted into the stand utilizing a move-and-push tool. Additionally, the radial arms were connected to the shaft, and the blade was positioned within the aperture provided in the radial arm; the Icewind rotor was positioned between the upper and lower radial arms, culminating in the assembled schematic diagram representing the hybrid vertical axis wind turbine as illustrated in Figures 3.2 and 3.3

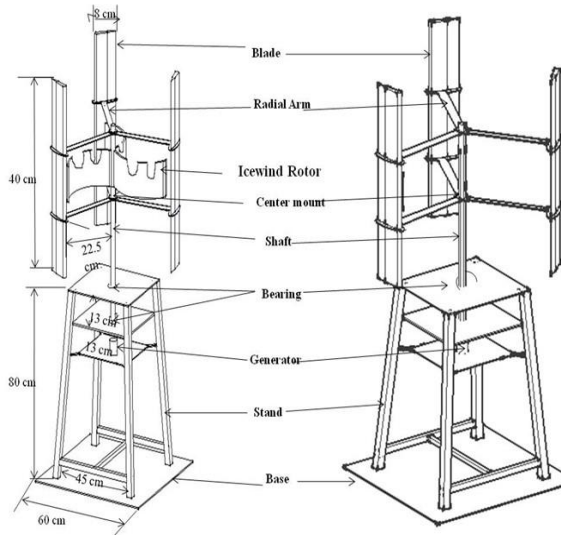


Figure 3.2: Schematic diagram of the (a) hybrid VAWT (b) H-Darrieus VAWT

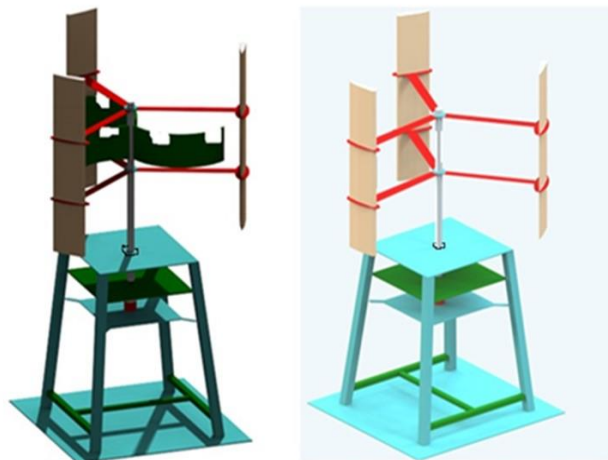


Figure 3.3: Computer Aid Design of the (a) hybrid VAWT (b) H-Darrieus VAWT

3.1 Experimental Setup

The experimental framework was established utilizing six electric standing fans, with the vertical axis wind turbine (VAWT) positioned at a distance of 100 cm from the fans, oriented in alignment with the fans, as depicted

in Figures 3.4 and 3.5. The separation between the blower and the VAWTs was systematically altered in increments of 5 cm to modulate the wind velocity, thereby facilitating the evaluation of the VAWTs under varying wind conditions. Wind velocity was quantified at

multiple locations, with the mean wind speed calculated for each designated point.



Figure 3.4: Experimental setup

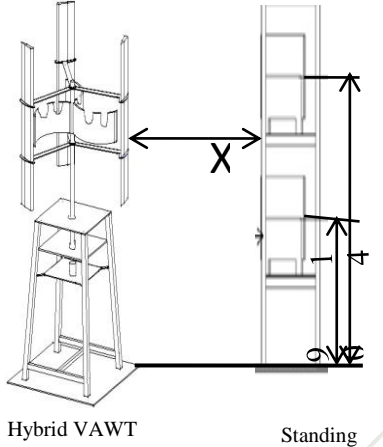


Figure 3.5: Symmetrical diagram of the experimental setup

The arrangement of the setup, characterized by a 3x2 configuration measuring 100 cm by 180 cm, is illustrated in Figure 3.5. The mean wind velocity was determined using an anemometer at ten distinct locations along a linear path aligned with the direction of the airflow produced by the fans, yielding an average speed of 4.77 m/s during operation. Subsequently, a horizontal distance of 100 cm was delineated between the fan and the turbine location ($X=100$ cm) along the wind trajectory, where the hybrid VAWT was positioned as indicated in Figure 3.5. The anemometer served to quantify wind velocity, while a tachometer was employed to assess revolutions

per minute (RPM) post-activation of the fans. A 0.3W LED load was incorporated, and measurements of both current and voltage were conducted. This protocol was reiterated for each position by incrementally increasing the distance. The H-Darrieus VAWT was substituted, with identical experimental parameters maintained.

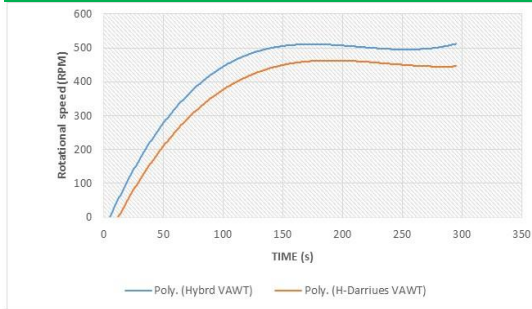
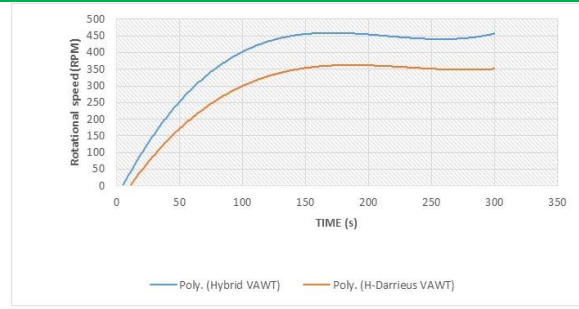
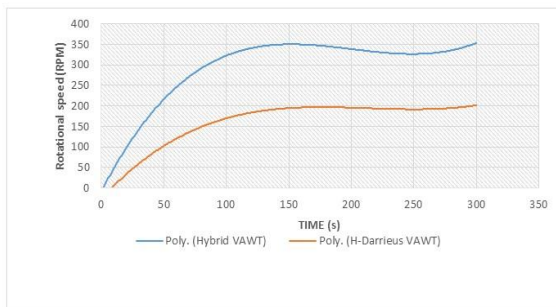
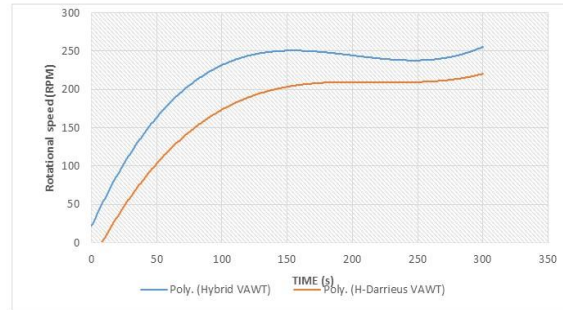
4.0 RESULTS AND DISCUSSION

The two experiments were performed under the same experimental conditions, one for the hybrid VAWT and another for the H-Darrieus VAWT. The two turbines' horizontal distance varied for four different wind speeds, i.e., $V = 4.80$ m/s, 4.50 m/s, 4.00 m/s, and 3.80 m/s, respectively.

4.1 Variation of Rotational Speed against Time

The temporal measurement utilizing a stopwatch commenced instantaneously upon the activation of the stationary fans, as delineated. Figure 4.1 illustrates the rotational velocities of both the hybrid Vertical Axis Wind Turbine (VAWT) and the H-Darrieus VAWT at a wind speed of 4.75 m/s. The revolutions per minute (RPM) for each turbine exhibit an upward trend over time until the peak RPM values of 500 and 450 are attained at $t = 155$ seconds and $t = 1655$ seconds, respectively. After reaching these apex RPM values, the rotational speeds attain a state of stabilization (constancy). The apex RPM recorded for the hybrid VAWT is 11 % superior to that of the H-Darrieus VAWT under identical experimental parameters. Figure 4.2 indicates that the hybrid VAWT initiated rotation before the H-Darrieus VAWT, with a temporal discrepancy of 15 seconds. At a wind speed of 4.50 m/s, the documented results reveal that the maximum rotational velocity of the hybrid VAWT is 450 at $t = 140$ seconds, whereas the H-Darrieus VAWT registers 350 at $t = 155$ seconds. The results depicted in Figure 4.2 demonstrate that the hybrid VAWT surpasses the H-Darrieus VAWT by 28.6 % in RPM.

In a similar vein, Figures 4.3 and 4.4 present the rotational speed per minute (RPM) for both the hybrid VAWT and H-Darrieus VAWT at horizontal distances of wind speed of 4.0 and 3.80 m/s, respectively. An analysis of these figures (4.3 and 4.4) reveals that the hybrid VAWT significantly outperforms the H-Darrieus VAWT in terms of RPM. The findings indicate that the RPM escalates by 75 % and 14 %, respectively, when compared to the H-Darrieus VAWT positioned similarly and subjected to the same experimental conditions.

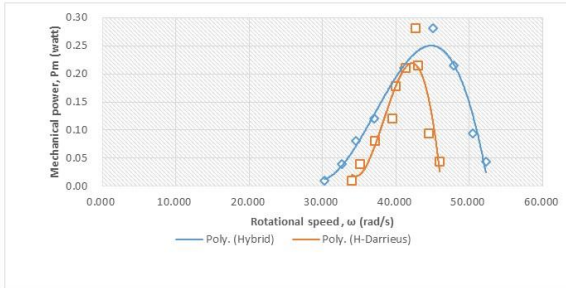
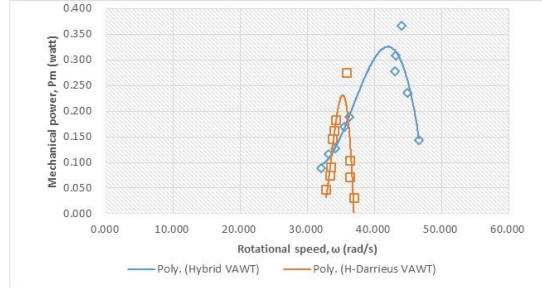
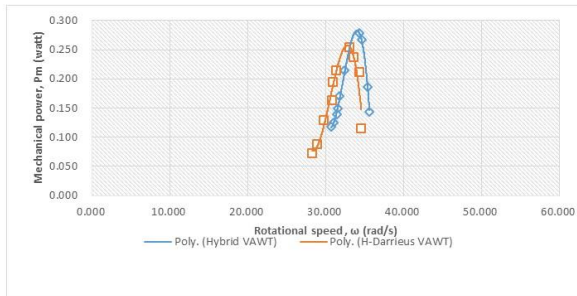
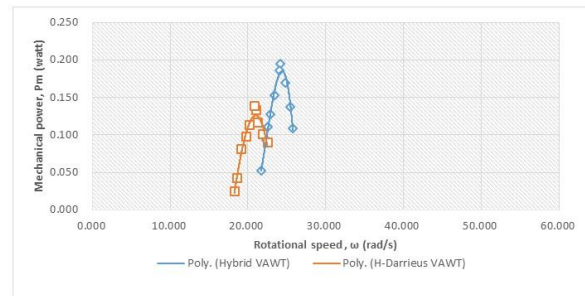
Figure 4.1: Rotational speed against time for Hybrid VAWT and H-Rotor VAWT for $V=4.75$ m/sFigure 4.2: Rotational speed against time for Hybrid VAWT and H-Rotor VAWT for $V=4.50$ m/sFigure 4.3: Rotational speed against time for Hybrid VAWT and H-Rotor VAWT for $V=4.00$ m/sFigure 4.4: Rotational speed against time for Hybrid VAWT and H-Rotor VAWT for $V=3.80$ m/s

4.2. Mechanical Power (P_m) against Rotational Speed (ω)

Figures 4.5–4.8 elucidate the mechanical power values in comparison between the hybrid Vertical Axis Wind Turbine (VAWT) and the H-Darrieus VAWT at specified positions of $V = 4.80$ m/s, 4.50 m/s, 4.00 m/s, and 3.80 m/s. The results, exhibiting a consistent trend, were derived for Figures 4.5 through 4.8. Figure 4.5 delineates the correlation between mechanical power and rotational speed (ω) for both the hybrid VAWT and the H-Darrieus VAWT positioned at $V = 4.80$ m/s. The observations recorded in Figure 4.5 indicate that the hybrid VAWT has achieved a peak mechanical power value of 0.28 W at a rotational speed (ω) of 45.021 rad/s. In contrast, the maximum mechanical power of the H-Darrieus VAWT, situated in the same location and subjected to identical experimental conditions, is 0.14 W at a rotational speed (ω) of 41.326 rad/s, as illustrated in Figure 4.5. These findings indicate that the hybrid VAWT exhibits an enhancement of 100% in maximum mechanical power compared to the H-Darrieus VAWT at $V = 4.80$ m/s. Figure 4.6 contrasts the mechanical power values between the hybrid VAWT and the H-Darrieus VAWT situated at a position of 105 cm. The results indicate that the hybrid VAWT recorded a maximum mechanical power of 0.4 W at a rotational speed (ω) of 43.993 rad/s, surpassing that of the H-Darrieus VAWT, whose

maximum mechanical power is 0.275 W at a rotational speed (ω) of 35.842 rad/s. The results at $V = 4.60$ m/s reveal that the hybrid VAWT outperforms the H-Darrieus VAWT by 45.5% . The previously mentioned increase in mechanical power is attributed to the icewind rotor, which enhances the turbine's operational speed.

Figure 4.7 illustrates the mechanical power values for the hybrid VAWT and H-Darrieus VAWT at a distance of $V = 4.00$ m/s. It is observed that the hybrid VAWT exhibits a higher mechanical power output compared to the H-Darrieus VAWT. The results demonstrate that the maximum mechanical power values achieved by the hybrid VAWT and the H-Darrieus VAWT are 0.279 W at a rotational speed (ω) of 34.237 rad/s and 0.255 W at a rotational speed (ω) of 20.068 rad/s, respectively. In comparison, the maximum mechanical power value for the hybrid VAWT is 9.4% greater than that of the H-Darrieus VAWT. Correspondingly, the results presented in Figure 4.8 for $V = 3.80$ m/s indicate that the mechanical power value of the hybrid VAWT increases by 40.3% relative to the H-Darrieus VAWT under analogous experimental conditions. The maximum mechanical power values recorded for the hybrid VAWT and H-Darrieus VAWT at $V = 3.80$ m/s are 0.195 W at a rotational speed (ω) of 24.174 rad/s and 0.139 W at a rotational speed (ω) of 20.870 rad/s, respectively.

Figure 4.5: Mechanical power against Rotational speed (ω) for Hybrid VAWT and H-Rotor VAWT for $V = 4.80$ m/sFigure 4.6: Mechanical power against Rotational speed (ω) for Hybrid VAWT and H-Rotor VAWT for $V = 4.50$ m/sFigure 4.7: Mechanical power against Rotational speed (ω) for Hybrid VAWT and H-Rotor VAWT for $V = 4.00$ m/sFigure 4.8: Mechanical power against Rotational speed (ω) for Hybrid VAWT and H-Rotor VAWT for $V = 3.80$ m/s

Figures 4.5-4.8 illustrate the correlation between mechanical power and rotational speed of the Vertical Axis Wind Turbine (VAWT). The enhancement in operational efficiency for the hybrid VAWT can be attributed to the Icewind rotor that is integrated with the turbine. The suboptimal rotational velocities output of the H-Darrieus VAWT can be ascribed to the radial arms (supporting struts) inherent to the H-Darrieus design. The presence of supporting struts within the H-Darrieus VAWT has adversely influenced the power output of the turbine by introducing additional drag (parasitic drag), thereby diminishing the overall performance of the H-Darrieus VAWT (Mohammed et al., 2021).

The Darrieus turbine currently encounters two significant challenges: subpar performance under low wind speed conditions and issues related to overspeed regulation. These critical concerns necessitate immediate scrutiny and actionable remediation strategies. Previous endeavors have yielded potential solutions; however, the intricacy and associated costs have constrained their applicability in commercial settings. In addressing these challenges, it is imperative to "consider low cost, increased starting torque at low wind speeds, sustained rotation, and the ability to regulate the rotor's rotational speed exceeding the rated RPM." (Kumar et al., 2019). The decline in lift is further aggravated by an elevated Angle of Attack (Ismail et al., 2020). The insufficient lift generated fails to produce the requisite torque necessary to surmount inertial and drivetrain resistance (Moreira et al., 2020), thus inhibiting rotation at low wind velocities. Relying exclusively on lift force to generate torque at low wind speeds proves to be impractical for a Darrieus

turbine. Prior investigations substantiate this assertion through wind tunnel experiments and empirical field tests (Shahzad et al., 2022). To mitigate the challenge of inadequate lift, substantial drag force can be harnessed to generate torque at low wind speeds, exemplified by the Savonius rotor. The Savonius rotor engenders drag and subsequently converts it into torque, wherein the magnitude is contingent upon the differential drag force experienced by the concave and convex sections of the blade (Kashem et al., 2021).

5.0 CONCLUSIONS

In this scholarly article, Vertical Axis Wind Turbines (VAWTS) have been meticulously designed, fabricated, and subjected to rigorous testing. The findings indicated that the rotational speed and mechanical power exhibited enhancements under identical experimental conditions for the hybrid VAWT, achieving percentages of (11.0 %, 28.6%, 75.0 %, 14.0 %) and (100 %, 45.5 %, 9.4%, and 40.3 %), respectively, in contrast to those of the Horizontal Darrieus VAWT. The indicated percentage increase demonstrates that the hybrid vertical-axis wind turbine substantially outperforms the traditional vertical-axis wind turbine. The integration of the Icewind rotor (Savonius Rotor) with the Horizontal Darrieus VAWT (hybrid VAWT) results in enhanced self-starting capabilities and superior performance in the evaluated parameters compared to the conventional Horizontal Darrieus VAWT.

ACKNOWLEDGMENTS

The authors thank the Tertiary Education Trust Fund

(TETFUND) for the Research Grant allocated through the Federal College of Education (Technical), Gusau, Zamfara State, Nigeria.

REFERENCES

- Akermi, N., Bacha, M. R. A., Benouar, A., & Khorsi, A. (2023). Power Prediction of Tandem Wind Rotor: Applied to Different Climatic Zones. *CFD Letters*, 15(4), 80–91. <https://doi.org/10.37934/cfdl.15.4.8091>
- Ali, N. M., A. K., A. H., & Aljabair, S. (2020). The Effect of Darrieus and Savonius Wind Turbines' Position on the Performance of the Hybrid Wind Turbine at Low Wind Speed. *International Journal of Mechanical Engineering and Technology (IJMET)*, 11(2), 56–72. <https://doi.org/10.34218/ijmet.11.2.2020.006>
- Ayodele E. G., Okolie C. J., and M. O. A. (2019). An Assessment of the Reliability of the NIGNET Data. *Nigerian Journal of Environmental Sciences and Technology (NIJEST)*, 3(1), 18–29. www.nijest.com%0AISSN
- Chaudhuri, A., Datta, R., Kumar, M. P., Davim, J. P., & Pramanik, S. (2022). Energy Conversion Strategies for Wind Energy Systems: Electrical, Mechanical, and Material Aspects. *Materials*, 15(3), 1–34. <https://doi.org/10.3390/ma15031232>
- Didane, D. H., Behery, M. R., Al-ghriybah, M., & Manshoor, B. (2024). Recent Progress in Design and Performance Analysis of Vertical-Axis Wind Turbines (VAWTs) - A Comprehensive Review. April, 1–31. <https://doi.org/10.20944/preprints202404.1310.v1>
- Dupré, A., Drobinski, P., Badosa, J., Briard, C., & Plougonven, R. (2019). Air Density Induced Error on Wind Energy Estimation. *Annales Geophysicae Discussions*, 1(July), 1–10.
- Fan, J., Meng, J., Ludescher, J., Chen, X., Ashkenazy, Y., Kurths, J., Havlin, S., & Schellnhuber, H. J. (2021). Statistical physics approaches to the complex Earth system. *Physics Reports*, 896, 1–84. <https://doi.org/10.1016/j.physrep.2020.09.005>
- Gwani, M., Buhari, M., Kangiwa, U. M., & Danyaro, J. (2020). Design, Fabrication, and Performance Evaluation of a Hybrid Vertical Axis Wind Turbine. *International Journal for Modern Trends in Science and Technology*, 6(6), 80–86. <https://doi.org/10.46501/ijmtst060618>
- Hidayanti, F., Wati, E. K., & Untoro, P. (2020). Design of Savonius-Darrieus, a Hybrid Wind Turbine. *International Journal of Management and Humanities (IJMH)* ISSN: 44(7), 107–109. <https://doi.org/10.35940/ijmh.G0724.034720>
- Homzah, O. F., Widagdo, T., Mardiana, Asrofi, I., & Pratama, D. A. (2021). Prototype of Small Savonius Wind Turbine. *Proceedings of the 4th Forum in Research, Science, and Technology (FIRST-T1-T2-2020)*, 7, 208–213. <https://doi.org/10.2991/ahe.k.210205.037>
- Ismail, N. A., Kaisan, M. U., Balogun, M. B., Abdullahi, M. B., Faru, F. T., & Ibrahim, I. U. (2020). Effect of Angle of Attack on Lift, Drag, Pitching Moment, and Pressure Distribution of NACA 4415 Wing. *Journal of Science Technology and Education*, 8(1).
- Kalmikov, A. (2017). *Wind Power Fundamentals. Wind Energy Engineering: A Handbook for Onshore and Offshore Wind Turbines*, April 17–24. <https://doi.org/10.1016/B978-0-12-809451-8.00002-3>
- Kashem, S. B. A., Chowdhury, M. E. H., Majid, M. E., Ashraf, A., Hasan-Zia, M., Nashbat, M., Kunju, A., & Esmaeili, A. (2021). A Comprehensive Review and the Efficiency Analysis of Horizontal and Vertical Axis Wind Turbines. *European Journal of Sustainable Development Research*, 5(3), em0163. <https://doi.org/10.21601/ejosdr/11001>
- Methal, Z., Aat, S., Hj, D., Mra, R., & Mr, S. (2022). Improvement of Hybrid Vertical Axis Wind Turbine Performance for Low Wind Speed Conditions. *PERINTIS EJournal*, 12(1), 42–55.
- Mohammed, G., Ibrahim, A., Mohammed Kangiwa, U., & Benjamin Wisdom, J. (2021). Design and Testing of Building Integrated Hybrid Vertical Axis Wind Turbine. *Journal of Electrical and Electronic Engineering*, 9(3), 69. <https://doi.org/10.11648/j.jee.20210903.12>
- Mojica, E. E., Fabay, C. M., Kehinde, F., & Tenorio, J. L. (2019). Design and development of an integrated Savonius and darrieus small scale vertical axis wind turbine for power generation. *IOP Conference Series: Earth and Environmental Science*, 291(1). <https://doi.org/10.1088/1755-1315/291/1/012041>
- Mokhena, T., Mochane, M., Tshwafo, M., Linganiso, L., Thekisoe, O., & Songca, S. (2016). We are IntechOpen, the world's leading publisher of Open Access books. Built by scientists, for scientists, TOP 1 %. *Intech*, 1(1), 225–240. <https://www.intechopen.com/books/advanced-biometric-technologies/liveness-detection-in-biometrics>
- Moreira, J. L. R., Mesquita, A. L. A., Araujo, L. F., Galhardo, M. A. B., Vaz, J. R. P., & Pinho, J. T. (2020). Experimental investigation of drivetrain resistance applied to small wind turbines. *Renewable Energy*, 153, 324–333. <https://doi.org/10.1016/j.renene.2020.02.014>
- Obada, D. O., Muhammad, M., Tajiri, S. B., Kekung, M. O., Abolade, S. A., Akinpelu, S. B., & Akande, A. (2024). A review of renewable energy resources in Nigeria for climate change mitigation. *Case Studies in Chemical and Environmental Engineering*, 9(February), 100669.



<https://doi.org/10.1016/j.cscee.2024.100669>

Salazar Marin, E. A., & Rodríguez, A. F. (2019). Design, assembly, and experimental tests of a Savonius-type wind turbine. *Scientia et Technica*, 24(3), 397–407. <https://doi.org/10.22517/23447214.20411>

Sarkar, M. R., Julai, S., Tong, C. W., Uddin, M., Romlie, M. F., & Shafiullah, G. M. (2020). Hybrid pitch angle controller approaches for stable wind turbine power under variable wind speed. *Energies*, 13(14). <https://doi.org/10.3390/en13143622>

Shahzad, A., Defence, A., Academy, F., Akram, F., Irtiza, S., & Shah, A. (2022). Design optimization of Double-Darrieus hybrid vertical axis wind turbine. *Ocean Engineering*, 242(06), 1–20. <https://doi.org/10.1016/j.oceaneng.2022.111171>

Wiens, M., Frahm, S., Thomas, P., & Kahn, S. (2021). Holistic simulation of wind turbines with a fully aero-elastic and electrical model. *Forschung Im Ingenieurwesen/Engineering Research*, 85(2), 417–424. <https://doi.org/10.1007/s10010-021-00479-6>